Cognitive radios are viewed as intelligent systems that can self-learn from their surrounding environments and auto-adapt their operating parameters in real time to improve spectrum efficiency. In this paper, we have developed an RL-based framework that exploits the cognitive radios' capabilities to enable effective OSA, thus improving the efficiency of spectrum utilization. The proposed learning technique does not require prior knowledge of the environment's characteristics and dynamics, yet it can still achieve high performance by learning from interaction with the environment.

REFERENCES

[1] *Spectrum Policy Task Force (SPTF), Report of the Spectrum Efficiency WG, Rep. ET Docket no. 02-135*, FCC, Washington, DC, Nov. 2002.

[2] M. Vilimpoc and M. McHenry, Dupont circle spectrum utilization during peak hours, 2006. [Online]. Available: www.newamerica.net/files/archive/Doc_File_183_1.pdf

[3] A. Ghasemi and E. S. Sousa, "Interference aggregation in spectrum-sensing cognitive wireless networks," *IEEE J. Sel. Topics Signal Process.*, vol. 2, no. 1, pp. 41–56, Feb. 2008.

[4] Z. Quan, S. Cui, and A. H. Sayed, "Optimal linear cooperation for spectrum sensing in cognitive radio networks," *IEEE J. Sel. Topics Signal Process.*, vol. 2, no. 1, pp. 28–40, Feb. 2008.

[5] H. Su and X. Zhang, "Cross-layer based opportunistic MAC protocols for QoS provisionings over cognitive radio wireless networks," *IEEE J. Sel. Areas Commun.*, vol. 26, no. 1, pp. 118–129, Jan. 2008.

[6] C.-T. Chou, S. Shankar, H. Kim, and K. G. Shin, "What and how much to gain by spectrum agility," *IEEE J. Sel. Areas Commun.*, vol. 25, no. 3, pp. 576–588, Apr. 2007.

[7] S. Srinivasa and S. A. Jafar, "Cognitive radio networks: How much spectrum sharing is optimal?" in *Proc. IEEE GLOBECOM*, Nov. 2007, pp. 3149–3153.

[8] Z. Ji and K. J. R. Liu, "Belief-assisted pricing for dynamic spectrum allocation in wireless networks with selfish users," in *Proc. IEEE SECON*, Sep. 2006, vol. 1, pp. 119–127.

[9] Z. Ji and K. J. R. Liu, "Multi-stage pricing game for collusion-resistant dynamic spectrum allocation," *IEEE J. Sel. Areas Commun.*, vol. 26, no. 1, pp. 182–191, Jan. 2008.

[10] S. Delaere and P. Ballon, "Flexible spectrum management and the need for controlling entities for reconfigurable wireless systems," in *Proc. IEEE DySPAN*, Apr. 2007, pp. 347–362.

[11] Y. T. Hou, Y. Shi, and H. D. Sherali, "Spectrum sharing for multi-hop networking with cognitive radios," *IEEE J. Sel. Areas Commun.*, vol. 26, no. 1, pp. 146–155, Jan. 2008.

[12] A. Ginsberg, J. D. Poston, and W. D. Horne, "Toward a cognitive radio architecture: Integrating knowledge representation with software defined radio technologies," in *Proc. IEEE MILCOM*, Oct. 2006, pp. 1–7.

[13] S. Yarkan and H. Arslan, "Exploiting location awareness toward improved wireless system design in cognitive radio," *IEEE Commun. Mag.*, vol. 46, no. 1, pp. 128–136, Jan. 2008.

[14] Z. Han, C. Pandana, and K. J. R. Liu, "Distributive opportunistic spectrum access for cognitive radio using correlated equilibrium and no-regret learning," in *Proc. IEEE WCNC*, Mar. 2007, pp. 11–15.

[15] K. E. Nolan, P. Sutton, and L. E. Doyle, "An encapsulation for reasoning, learning, knowledge representation, and reconfiguration cognitive radio elements," in *Proc. Int. Conf. Cogn. Radio Oriented Wireless Netw. Commun.*, Jun. 2006, pp. 1–5.

[16] H. Kim and K. G. Shin, "Fast discovery of spectrum opportunities in cognitive radio networks," in *Proc. IEEE DySPAN*, Oct. 2008, pp. 1–12.

[17] H. Kim and K. G. Shin, "Efficient discovery of spectrum opportunities with MAC-layer sensing in cognitive radio networks," *IEEE Trans. Mobile Comput.*, vol. 7, no. 5, pp. 533–545, May 2008.

[18] U. Berthold, M. Van Der Schaar, and F. K. Jondral, "Detection of spectral resources in cognitive radios using reinforcement learning," in *Proc. IEEE DySPAN*, Oct. 2008, pp. 1–5.

[19] M. Maskery, V. Krishnamurthy, and Q. Zhao, "Decentralized dynamic spectrum access for cognitive radios: Cooperative design of a non-cooperative game," *IEEE Trans. Commun.*, vol. 57, no. 2, pp. 459–469, Feb. 2009.

[20] J. Unnikrishnan and V. V. Veeravalli, "Dynamic spectrum access with learning for cognitive radio," in *Proc. Asilomar Conf. Signals Syst. Comput.*, Oct. 2008, pp. 103–107.

[21] J. Unnikrishnan and V. V. Veeravalli, "Cooperative sensing for primary detection in cognitive radio," *IEEE J. Sel. Topics Signal Process.*, vol. 2, no. 1, pp. 18–27, Feb. 2008.

[22] H. Liu, B. Krishnamachari, and Q. Zhao, "Cooperation and learning in multiuser opportunistic spectrum access," in *Proc. IEEE ICC*, 2008, pp. 487–492.

[23] K. Liu and Q. Zhao, "Distributed learning in cognitive radio networks: Multi-armed bandit with distributed multiple players," in *Proc. IEEE Int. Conf. Acoust., Speech, Signal Process.*, 2010.

[24] Y. Chen, Q. Zhao, and S. Ananthram, "Joint design and separation principle for opportunistic spectrum access in the presence of sensing errors," *IEEE Trans. Inf. Theory*, vol. 54, no. 5, pp. 2053–2071, May 2008.

[25] Y. Chen, Q. Zhao, and A. Swami, "Joint design and separation principle for opportunistic spectrum access in the presence of sensing errors," *IEEE Trans. Inf. Theory*, vol. 54, no. 5, pp. 2053–2071, May 2008.

[26] Q. Zhao, S. Geirhofer, L. Tong, and B. M. Sadler, "Opportunistic spectrum access via periodic channel sensing," *IEEE Trans. Signal Process.*, vol. 56, no. 2, pp. 785–796, Feb. 2008.

[27] R. S. Sutton and A. G. Barto, *Reinforcement Learning*. Cambridge, MA: MIT Press, 1998.

A Transceiver Design Based on Uniform Channel Decomposition and MBER Vector Perturbation

W. Yao, S. Chen, and L. Hanzo

***Abstract*—Uniform channel decomposition (UCD), as an improvement of geometric mean decomposition (GMD), is capable of decomposing a multiple-input–multiple-output (MIMO) channel into multiple subchannels having an identical capacity. Vector precoding (VP) is a powerful scheme, which is capable of mitigating multiuser interference (MUI) at the transmitter, provided that the channels of the users are known. In this paper, a novel joint transceiver design based on the UCD and the minimum bit error rate (MBER) VP principles is proposed for MIMO systems, in which the precoding and equalization matrices are calculated by UCD, whereas the perturbation vector is chosen to minimize the system's bit error ratio (BER). This UCD-MBER-VP transceiver design outperforms several state-of-the-art benchmark algorithms in terms of achievable BER performance without imposing an increased computational complexity, particularly for rank-deficient systems.**

***Index Terms*—Minimum bit error rate (MBER), multiple-input–multiple-output (MIMO), uniform channel decomposition (UCD), vector perturbation.**

I. INTRODUCTION

Multiple-input–multiple-output (MIMO) techniques are capable of offering high channel capacity in interference-free scenarios [1], albeit their achievable performance is limited by the multiuser interference (MUI). Nonetheless, the MUI can be mitigated either at the receiver [2]

Manuscript received November 5, 2009; revised March 2, 2010; accepted April 1, 2010. Date of publication April 22, 2010; date of current version July 16, 2010. This work was supported in part by the Engineering and Physical Sciences Research Council, U.K., and in part by the European Union under the auspices of the Optimix Project. The review of this paper was coordinated by Prof. W. A. Hamouda.

The authors are with the School of Electronics and Computer Science, University of Southampton, SO17 1BJ Southampton, U.K. (e-mail: wy07r@ecs.soton.ac.uk; sqc@ecs.soton.ac.uk; lh@ecs.soton.ac.uk).

Color versions of one or more of the figures in this paper are available online at http://ieeexplore.ieee.org.

Digital Object Identifier 10.1109/TVT.2010.2048439

or at the transmitter [3], as well as at both the transmitter and the receiver [4], with the latter approach leading to a joint MIMO transceiver design. A nonlinear transceiver design based on geometric mean decomposition (GMD) was proposed in [5]. The GMD is capable of beneficially diagonalizing the MIMO channel matrix, leading to identical diagonal elements and, hence, offering identical subchannel gains. Later, uniform channel decomposition (UCD) was proposed in [6] as an improvement to GMD. The UCD maintains the highest possible capacity at any SNR, and it achieves the maximal diversity gain [6]. The precoder design in [5] and [6] constitutes a Tomlinson–Harashima style precoder (THP) [7], which is a specific implementation of the dirty paper coding (DPC) principle [8]. THP designs are generally outperformed by vector precoding (VP) schemes [3], [9], where each receiver employs a modulo operation [9], but the latter imposes a higher computational complexity.

The VP can be interpreted as a multiuser transmission (MUT) technique, which appropriately chooses the perturbation vector [9] to mitigate the MUI. This technique was found to be powerful in terms of approaching the rate region of DPC [8], and it is also capable of achieving better bit error ratio (BER) performance than other MUT techniques. The zero-forcing-based VP principle was proposed for MUT preprocessing in [9], whereas the MMSE-based VP (MMSE-VP) solution was derived later in [3] for transmission in frequency flat-fading multiuser scenarios with the aid of a multiantenna transmitter. An improved MMSE-VP design (ImMMSE-VP) was proposed in [10], which calculates the precoding matrix using the MMSE-VP method and determines the perturbation vector based on the minimum bit error rate (MBER) criterion. The work in [9] suggested that the search for the optimal perturbation vector can be implemented by using the so-called sphere encoding algorithm. Several search algorithms were later proposed in [11] and [12], which are capable of achieving near-optimal performance while significantly reducing the computational complexity. These reduced-complexity search algorithms make the implementation of the VP solution more feasible in practice.

The solution presented in [4] extended the idea of a joint transmitter and receiver design, which was first proposed in [5], to a GMD-aided MMSE-VP (GMD-MMSE-VP) transceiver design. In this paper, we propose a transceiver design based on the UCD and the MBER vector perturbation (UCD-MBER-VP). Our novel contributions are as follows.

1) Although the authors of [6] proposed a UCD-based THP design (UCD-THP), to the best of our knowledge, no UCD-aided VP transceiver design has been proposed to date in the open literature. We, hence, propose a joint transceiver design by intrinsically amalgamating the UCD with vector perturbation.
2) The MMSE criterion is popularly adopted in VP-related schemes. However, since the bit error rate (BER) is the ultimate system-performance indicator, schemes designed by minimizing the BER criterion are attractive. We thus invoked the MBER criterion for our transceiver design to improve its overall BER performance and derived a novel solution based on the MBER criterion.
3) All the benchmark designs, namely, the MMSE-VP design proposed in [3], the ImMMSE-VP scheme advocated in [10], the UCD-THP algorithm contrived in [6], and the GMD-MMSE-VP design proposed in [4], assumed that the number of transmit antennas is equal to or higher than the number of users, that is, they all avoid the discussion of practical rank-deficient scenarios, where the number of users supported is more than the number of transmit antennas employed. We demonstrate that our design outperforms all the benchmark designs, particularly in the challenging rank-deficient scenario. In such challenging scenarios, conventional algorithms encounter error floors, whereas the proposed scheme does not.
4) We showed that our intrinsically amalgamated design approach imposes a similar computational complexity to that of classic benchmark schemes.

For ease of reference, the abbreviations used to represent all the algorithms compared in this paper are briefly explained as follows.

1) MMSE-VP [3]: The precoding matrix and the perturbation vector are chosen to minimize the system's mean square error (MSE). No equalization matrix is employed; hence, no cooperation is required among the users. This is an MUT technique.
2) ImMMSE-VP [10]: The precoding matrix is calculated using the MMSE-VP method, and the perturbation vector is determined based on the MBER criterion. No equalization matrix is used; hence, no cooperation is required among the users. This is an MUT technique.
3) UCD-THP [6]: The precoding and equalization matrices are calculated by the UCD, whereas the modulo operation [3] maps the effective symbols into the fundamental Voronoi region [3] so that the total transmit power is constrained. This is a joint transceiver design method. Both the transmitter and the receiver require to know the channel state information (CSI).
4) GMD-MMSE-VP [4]: The precoding and equalization matrices are calculated by the GMD, whereas the perturbation vector is chosen to minimize the system's MSE. This is a joint transceiver-design technique. Both the transmitter and the receiver require knowledge of the CSI.
5) UCD-MBER-VP: In the proposed algorithm, the precoding and equalization matrices are calculated by the UCD, whereas the perturbation vector is specifically chosen based on the MBER criterion. As this is a joint transceiver design method, the CSI is required at both the transmitter and the receiver.

The rest of this paper is structured as follows: In Section II, the MIMO system model is introduced, whereas Section III details the proposed UCD-MBER-VP transceiver design. The simulation results are presented in Section IV to compare our proposed design to several existing benchmark schemes. Finally, we conclude our discourse in Section V.

II. Multiple-Input–Multiple-Output System Model

The schematic of the MIMO system considered is depicted in Fig. 1, where the transmitter equipped with N antennas transmits the K users' data streams[1] to the receiver employing K receive antennas and K modulo devices [9]. Frequency flat-fading channels are considered, and the channel matrix $\mathbf{H}$ of the system is given by

$$\mathbf{h} = [\mathbf{h}_1 \quad \mathbf{h}_2 \quad \cdots \quad \mathbf{h}_K] \tag{1}$$

where $\mathbf{h}_k = [h_{1,k} \quad h_{2,k} \quad \cdots \quad h_{N,k}]^T$, $1 \le k \le K$, and $(\bullet)^T$ is the transpose operator. The channel impulse response taps $h_{i,k}$ for $1 \le k \le K$ and $1 \le i \le N$ are independent of each other and obey the complex-valued Gaussian distribution with $E[|h_{i,k}|^2] = 1$, where $E[\bullet]$ denotes the expectation operator. The K-element original information symbol vector is given by $\mathbf{x} = [x_1 \quad x_2 \quad \cdots \quad x_K]^T$, where x_k denotes the kth information symbol, and $E[\mathbf{x}\mathbf{x}^H] = \sigma_x^2 \mathbf{I}_K$, with $\mathbf{I}_K$ denoting the $(K \times K)$-element identity matrix and $(\bullet)^H$ the

[1]The technique is equally applicable to a single-user K-layered spatial multiplexing-based MIMO system.

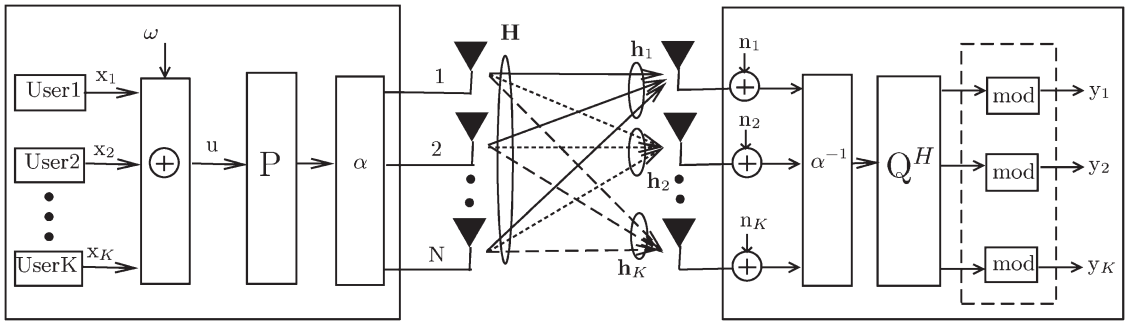

Fig. 1. Schematic of the MIMO system, where the transmitter employing N transmit antennas communicates with the receiver having K receive antennas and K modulo devices [9].

Hermitian operator. The original symbol vector $\mathbf{x}$ is then perturbed to generate the K-element perturbed vector $\mathbf{u}$, as given by

$$\mathbf{u} = \mathbf{x} + \boldsymbol{\omega} \tag{2}$$

where $\boldsymbol{\omega}$ is a complex-valued perturbation vector, which can be appropriately chosen to minimize the total transmission power [9], the MSE [3], or the BER, as proposed in this paper. The channel's white noise vector $\mathbf{n}$ is defined by $\mathbf{n} = [n_1 \quad n_2 \quad \cdots \quad n_K]^T$, where n_k, $1 \leq k \leq K$ is a complex-valued Gaussian random process with zero mean, and $E[|n_k|^2] = 2\sigma_n^2 = N_o$. The $(N \times K)$-element precoding matrix $\mathbf{P}$ in Fig. 1 is given by

$$\mathbf{P} = [\mathbf{p}_1 \quad \mathbf{p}_2 \quad \cdots \quad \mathbf{p}_K] \tag{3}$$

where $\mathbf{p}_k$, $1 \leq k \leq K$ is the precoder's coefficient vector for the kth user's data stream. Given a total radiated power E_T at the transmitter, an appropriate scaling factor should be used to fulfill this transmit power constraint, which is defined as [9], [13]

$$\alpha = \sqrt{E_T / \|\mathbf{P}\mathbf{u}\|^2}. \tag{4}$$

The scaling factor α is transmitted to the receiver as side information, where the reciprocal of α, namely, α^{-1}, is used to scale the received signal for maintaining unity-gain transmission. The received signal vector $\hat{\mathbf{y}} = [\hat{y}_1 \quad \hat{y}_2 \quad \cdots \quad \hat{y}_K]^T$ before the modulo operation is given by

$$\hat{\mathbf{y}} = \mathbf{Q}^H \mathbf{H}^T \mathbf{P}\mathbf{u} + \alpha^{-1}\mathbf{Q}^H\mathbf{n} \tag{5}$$

with the $(K \times K)$-element equalization matrix $\mathbf{Q}$ in Fig. 1 defined as $\mathbf{Q} = [\mathbf{q}_1 \quad \mathbf{q}_2 \quad \cdots \quad \mathbf{q}_K]$. The modulo operation in Fig. 1 invoked for $\hat{y}_k$, $1 \leq k \leq K$ is described by [9]

$$\mathrm{mod}_\tau(\hat{y}_k) = \hat{y}_k - \left\lfloor \frac{\Re[\hat{y}_k] + \tau/2}{\tau} \right\rfloor \tau - j \left\lfloor \frac{\Im[\hat{y}_k] + \tau/2}{\tau} \right\rfloor \tau \tag{6}$$

where $\Re[\bullet]$ and $\Im[\bullet]$ represent the real and imaginary parts, respectively, $j^2 = -1$, $\lfloor \bullet \rfloor$ denotes the largest integer less than or equal to its argument, and τ is a positive number [9]. If the M-point square-shaped Gray-coded quadrature amplitude modulation (QAM) constellation of

$$\left\{ \pm\frac{1}{2}, \ldots, \pm\frac{\sqrt{M}-1}{2} \right\} + j \left\{ \pm\frac{1}{2}, \ldots, \pm\frac{\sqrt{M}-1}{2} \right\}$$

is used, the modulo operation parameter can be set to $\tau = \sqrt{M}$ [3], [14]. Letting y_k, $1 \leq k \leq K$ denote the kth user's signal at the output of the modulo operator, we then have $y_k = \mathrm{mod}_\tau(\hat{y}_k)$; thus, the received signal vector $\mathbf{y} = [y_1 \quad y_2 \quad \cdots \quad y_K]^T$ after the modulo operation is given by

$$\mathbf{y} = \mathrm{mod}_\tau(\hat{\mathbf{y}}) \tag{7}$$

and y_k, $1 \leq k \leq K$ constitutes the sufficient statistics for the receiver to detect the transmitted information data symbol x_k, $1 \leq k \leq K$.

Given $\mathbf{x}$ and $\mathbf{H}$, the task of a joint transceiver design is to determine the perturbation vector $\boldsymbol{\omega}$, the precoding matrix $\mathbf{P}$, and the equalization matrix $\mathbf{Q}$ based on a specified criterion. Note that the VP principle [9], which is specified by the design of $\boldsymbol{\omega}$ and $\mathbf{P}$, as well as the modulo operation [see (6)], is a more effective means of mitigating the MUI than a MUT technique that relies only on the precoding matrix $\mathbf{P}$ to do so.

III. Uniform Channel Decomposition-Aided Minimum Bit Error Rate Vector Precoding Transceiver Design

For notational simplicity, we restrict our discourse to the 4-QAM scheme of $M = 4$. Its extension to high-order QAM schemes can be achieved by considering the minimum symbol error rate criterion, as in the multiuser detection case [15]. The UCD scheme [6] is used to design the precoding matrix $\mathbf{P}$ and the equalization matrix $\mathbf{Q}$, whereas the design of the perturbation vector $\boldsymbol{\omega}$ is based on the novel MBER criterion. Let us denote the singular value decomposition (SVD) [16] of $\mathbf{H}^*$ as $\mathbf{H}^* = \mathbf{U}\boldsymbol{\Lambda}\mathbf{V}^H$, where $(\bullet)^*$ denotes the conjugate operator, $\boldsymbol{\Lambda}$ is the $(O \times O)$-element diagonal matrix, whose diagonal elements $\{\lambda_o\}_{o=1}^O$ are the nonzero singular values of $\mathbf{H}^*$, $\mathbf{U}$ is an $(N \times O)$-element matrix, and $\mathbf{V}^H$ is an $(O \times K)$-element matrix.

We calculate the equalization matrix $\mathbf{Q}$ in Fig. 1 according to [6]

$$\mathbf{Q} = \mathbf{V}\boldsymbol{\Phi}\boldsymbol{\Omega}^H \tag{8}$$

where $\boldsymbol{\Phi}$ is a $(O \times O)$-element diagonal matrix, and $\boldsymbol{\Omega}$ is a $(K \times O)$-element matrix. As shown in [6], $\boldsymbol{\Phi}$ and $\boldsymbol{\Omega}$ can be obtained by following the approach in [17]. Explicitly, the diagonal elements $\{\phi_o\}_{o=1}^O$ of $\boldsymbol{\Phi}$ are found by the water-filling process as

$$\phi_o^2(\mu) = \left(\mu - \frac{\beta}{\lambda_o^2} \right)^+ \tag{9}$$

where β is defined as $\beta = 2\sigma_n^2/\sigma_x^2$, μ is chosen so that $\sum_{o=1}^O \phi_o^2(\mu) = O$, and $(a)^+ = \max\{0, a\}$. Let us now introduce $\boldsymbol{\Sigma} = \boldsymbol{\Lambda}\boldsymbol{\Phi}$. Then, $\boldsymbol{\Omega}$ is obtained with the aid of the GMD, as given in [6]

$$\left[\mathbf{U} \left[\begin{array}{c|c} \boldsymbol{\Sigma} & \mathbf{0}_{O\times(K-O)} \\ \hline & \sqrt{\beta}\mathbf{I}_K \end{array} \right] \right] = \mathbf{Q}_J \mathbf{R}_J \mathbf{P}_J^H \tag{10}$$

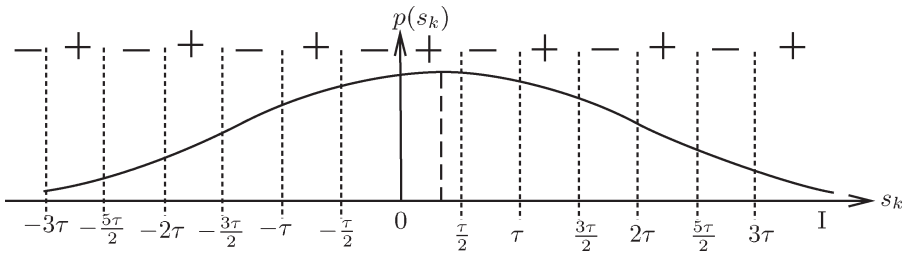

Fig. 2. PDF of the decision variable s_k.

where $\mathbf{R}_J$ is a $(K \times K)$-element upper triangular matrix having identical real-valued diagonal elements, $\mathbf{Q}_J$ is a $[(N+K) \times K]$-element semi-unitary matrix, and $\mathbf{P}_J$ is a $(K \times K)$-element unitary matrix. The matrix $\mathbf{\Omega}$ simply consists of the first O columns of $\mathbf{P}_J^H$.

The precoding matrix $\mathbf{P}$, on the other hand, is calculated according to [6]

$$\mathbf{P} = \mathbf{Q}_u \left(\mathbf{R}_J^H\right)^{-1} \tag{11}$$

where $\mathbf{Q}_u$ consists of the first N rows of $\mathbf{Q}_J$.

Having designed $\mathbf{P}$ and $\mathbf{Q}$, we describe the proposed VP design. The error probability encountered at the output of the receiver after the modulo operation of (7) for the in-phase component of the kth symbol is a function of the perturbation vector $\boldsymbol{\omega}$, which is defined by [18]

$$P_{e_I,k}(\boldsymbol{\omega}) = \text{Prob}\left\{\text{sgn}\left(\Re[x_k]\right)\Re[y_k] < 0\right\}. \tag{12}$$

Let us define the signed decision variable $s_k = \text{sgn}(\Re[x_k])\Re[\hat{y}_k]$, which has a mean of $c_R^{(k)} = \text{sgn}(\Re[x_k])\Re[\mathbf{q}_k^H \mathbf{h}_k^T \mathbf{P}(\mathbf{x}+\boldsymbol{\omega})]$, whereas $c_R^{(k)}$ is within the interval $(-\tau/2, \tau/2)$ due to the effect of the modulo operation, and the probability density function (pdf) is given by

$$p(s_k) = \frac{1}{\alpha^{-1}\sigma_n\sqrt{2\pi\mathbf{q}_k^H\mathbf{q}_k}} \exp\left(-\frac{\left(s_k - c_R^{(k)}\right)^2}{2\sigma_n^2\alpha^{-2}\mathbf{q}_k^H\mathbf{q}_k}\right). \tag{13}$$

Note that the decision areas are periodically extended in the s_k-axis, as illustrated in Fig. 2, where the intervals marked by $-$ are the erroneous decision areas having $\text{sgn}(\Re[x_k])\Re[y_k] < 0$, whereas the intervals marked by $+$ are the error-free areas, i.e., $\text{sgn}(\Re[x_k])\Re[y_k] > 0$.

Specifically, a decision error occurs when s_k falls into the intervals $[(2t+1)\tau/2, (t+1)\tau)$ for $-\infty < t < \infty$. Therefore, the BER of the in-phase component associated with the kth symbol is given by

$$\begin{aligned} P_{e_I,k}(\boldsymbol{\omega}) &= \sum_{t=-\infty}^{\infty} \int_{\frac{2t+1}{2}\tau}^{(t+1)\tau} p(s_k)ds_k \approx \int_{-\infty}^{-3\tau} p(s_k)ds_k \\ &+ \int_{\frac{5\tau}{2}}^{-2\tau} p(s_k)ds_k + \int_{-\frac{3\tau}{2}}^{-\tau} p(s_k)ds_k \\ &+ \int_{-\frac{\tau}{2}}^{0} p(s_k)ds_k + \int_{\frac{\tau}{2}}^{\tau} p(s_k)ds_k \\ &+ \int_{\frac{3\tau}{2}}^{2\tau} p(s_k)ds_k + \int_{\frac{5\tau}{2}}^{3\tau} p(s_k)ds_k \end{aligned} \tag{14}$$

where the approximation occurs as we approximate the integrations over all the error intervals in $(-\infty, -3\tau)$ and $(3\tau, +\infty)$ as the single integration over the interval $(-\infty, -3\tau)$. This approximation is accurate owing to the near symmetry of the pdf [see (13)] in the two regions of $(3\tau, +\infty)$ and $(-\infty, -3\tau)$. Furthermore, the last six integrals on the right-hand side of the approximation are generally much larger than the first term. We also justified this approximation by our intensive simulations, which is omitted here due to lack of space. Therefore, $P_{e_I,k}(\boldsymbol{\omega})$ can be expressed as

$$\begin{aligned} P_{e_I,k}(\boldsymbol{\omega}) \approx\ & Q\left(\frac{c_R^{(k)} + 3\tau}{\alpha^{-1}\sigma_n\sqrt{\mathbf{q}_k^H\mathbf{q}_k}}\right) + Q\left(\frac{-\frac{5\tau}{2} - c_R^{(k)}}{\alpha^{-1}\sigma_n\sqrt{\mathbf{q}_k^H\mathbf{q}_k}}\right) \\ & - Q\left(\frac{-2\tau - c_R^{(k)}}{\alpha^{-1}\sigma_n\sqrt{\mathbf{q}_k^H\mathbf{q}_k}}\right) + Q\left(\frac{-\frac{3\tau}{2} - c_R^{(k)}}{\alpha^{-1}\sigma_n\sqrt{\mathbf{q}_k^H\mathbf{q}_k}}\right) \\ & - Q\left(\frac{-\tau - c_R^{(k)}}{\alpha^{-1}\sigma_n\sqrt{\mathbf{q}_k^H\mathbf{q}_k}}\right) + Q\left(\frac{-\frac{\tau}{2} - c_R^{(k)}}{\alpha^{-1}\sigma_n\sqrt{\mathbf{q}_k^H\mathbf{q}_k}}\right) \\ & - Q\left(\frac{-c_R^{(k)}}{\alpha^{-1}\sigma_n\sqrt{\mathbf{q}_k^H\mathbf{q}_k}}\right) + Q\left(\frac{\frac{\tau}{2} - c_R^{(k)}}{\alpha^{-1}\sigma_n\sqrt{\mathbf{q}_k^H\mathbf{q}_k}}\right) \\ & - Q\left(\frac{\tau - c_R^{(k)}}{\alpha^{-1}\sigma_n\sqrt{\mathbf{q}_k^H\mathbf{q}_k}}\right) + Q\left(\frac{\frac{3\tau}{2} - c_R^{(k)}}{\alpha^{-1}\sigma_n\sqrt{\mathbf{q}_k^H\mathbf{q}_k}}\right) \\ & - Q\left(\frac{2\tau - c_R^{(k)}}{\alpha^{-1}\sigma_n\sqrt{\mathbf{q}_k^H\mathbf{q}_k}}\right) + Q\left(\frac{\frac{5\tau}{2} - c_R^{(k)}}{\alpha^{-1}\sigma_n\sqrt{\mathbf{q}_k^H\mathbf{q}_k}}\right) \\ & - Q\left(\frac{3\tau - c_R^{(k)}}{\alpha^{-1}\sigma_n\sqrt{\mathbf{q}_k^H\mathbf{q}_k}}\right) \end{aligned} \tag{15}$$

where $Q(\,)$ is the standard Gaussian error function. Hence, the average BER for the in-phase component of $\mathbf{y}$ at the receiver is given by

$$P_{e_I,\mathbf{x}}(\boldsymbol{\omega}) = \frac{1}{K}\sum_{k=1}^{K} P_{e_I,k}(\boldsymbol{\omega}). \tag{16}$$

Similarly, let $c_I^{(k)} = \text{sgn}(\Im[x_k])\Im[\mathbf{q}_k^H \mathbf{h}_k^T \mathbf{P}(\mathbf{x}+\boldsymbol{\omega})]$. Then, the BER of the quadrature-phase component for the kth symbol, which is denoted as $P_{e_Q,k}(\boldsymbol{\omega})$, can be derived by replacing $c_R^{(k)}$ with $c_I^{(k)}$ in (15). Then, the average BER for the quadrature-phase component of $\mathbf{y}$ at the receiver is given by

$$P_{e_Q,\mathbf{x}}(\boldsymbol{\omega}) = \frac{1}{K}\sum_{k=1}^{K} P_{e_Q,k}(\boldsymbol{\omega}). \tag{17}$$

Thus, the resultant average BER of 4-QAM signaling becomes

$$P_{e,\mathbf{x}}(\boldsymbol{\omega}) = \left(P_{e_I,\mathbf{x}}(\boldsymbol{\omega}) + P_{e_Q,\mathbf{x}}(\boldsymbol{\omega})\right)/2. \quad (18)$$

Hence, the optimal perturbation vector $\boldsymbol{\omega}_{\text{opt}}$ is determined by solving the following optimization problem:

$$\boldsymbol{\omega}_{\text{opt}} = \arg\min_{\boldsymbol{\omega}} P_{e,\mathbf{x}}(\boldsymbol{\omega}). \quad (19)$$

The perturbation vector $\boldsymbol{\omega}$ can be discrete valued [3] or continuous valued [10]. When only the discrete-valued selection is considered, we have

$$\boldsymbol{\omega} = \tau\boldsymbol{\zeta} \quad (20)$$

where $\boldsymbol{\zeta}$ is a complex-valued vector taking values from the set $\{a + jb\}$ with a and b being integers. Then, the optimization problem (19) is reduced to

$$\boldsymbol{\zeta}_{\text{opt}} = \arg\min_{\boldsymbol{\zeta}} P_{e,\mathbf{x}}(\boldsymbol{\zeta}). \quad (21)$$

The optimization problem (21) can readily be solved using the sphere encoding algorithm of [9] or using the reduced-complexity algorithms proposed in [11] and [12] at a slight performance degradation.

The computational requirements of the proposed UCD-MBER-VP design include the UCD operation, which has comparable computational complexity with the SVD [6], and the solution of the optimization problem [see (21)], which has a significantly higher complexity than the UCD. Thus, the computational complexity of the UCD-MBER-VP design is dominated by the search for the optimal discrete-valued MBER perturbation vector. Therefore, our design may be deemed to have a similar complexity to that of the GMD-MMSE-VP design in [4], the MMSE-VP algorithm in [3], and the ImMMSE-VP algorithm in [10], whose computational requirements are also dominated by the search of the corresponding optimal discrete-valued perturbation vectors.

More specifically, let N and K be the number of transmitter and receiver antennas, respectively, whereas $D_{\text{TheScheme}}$ denotes the extended constellation points visited when determining the discrete-valued perturbation vector [3], [4], [10] by the scheme considered. Then, the complexity of the ImMMSE-VP design [10] can be shown to be

$$C_{\text{ImMMSE-VP}} = (18KN + 73K + 6N + 4)D_{\text{ImMMSE-VP}} \quad (22)$$

whereas the complexity of the MMSE-VP design [3] can be evaluated as

$$C_{\text{MMSE-VP}} = \left(\frac{7}{3}K^3 + 13K^2 + 13K - 1\right) D_{\text{MMSE-VP}} + 9K^2N - 2K^2. \quad (23)$$

On the other hand, the complexity of the GMD-MMSE-VP design [4] can be calculated as

$$C_{\text{GMD-MMSE-VP}} = \left(\frac{7}{3}K^3 + 13K^2 + 13K - 1\right) \times D_{\text{GMD-MMSE-VP}} + 9K^2N - 2K^2 \quad (24)$$

whereas our proposed UCD-MBER-VP design has the complexity calculated as

$$C_{\text{UCD-MBER-VP}} = (9K^2 + 18KN + 71K + 6N + 4) \times D_{\text{UCD-MBER-VP}} + 8K^2 - K. \quad (25)$$

TABLE I
COMPUTATIONAL REQUIREMENTS OF THE FOUR DESIGNS FOR THE 4-QAM SYSTEM WITH $N = 4$ TRANSMIT ANTENNAS AND $K = 4$ RECEIVE ANTENNAS GIVEN SNR = 10 dB

Algorithm	GMD-MMSE-VP	MMSE-VP
Points visited	3214	3172
Complexity (Flops)	1,312,820	1,295,671
Algorithm	ImMMSE-VP	UCD-MBER-VP
Points visited	3248	2153
Complexity (Flops)	1,974,784	1,601,956

The computational requirements of these four designs are compared in Table I for the 4-QAM system employing $N = 4$ transmit and $K = 4$ receive antennas at SNR = 10 dB. It is clear that, in this case, the computational complexities of the search for perturbation vectors required by the GMD-MMSE-VP, the MMSE-VP, and the UCD-MBER-VP are similar, whereas the ImMMSE-VP imposes an approximately 1.5-times-higher computational complexity than that of the MMSE-VP. The UCD-THP design [6] benefits from a lower computational complexity, but it is outperformed by all the other designs in terms of its BER performance at high SNRs, as will be demonstrated by the simulation results presented in Section IV.

IV. SIMULATION RESULTS

We considered the MIMO system employing N transmit antennas and K receive antennas. The squared 4-QAM constellation of $\{\pm(1/2)\} + j\{\pm(1/2)\}$ was used; hence, we have $\tau = 2$ for the modulo operator [see (6)]. The received signals after the modulo operation [see (6)] were used to make decisions. The system's SNR was defined as SNR $= E_b/N_o$, where $E_b = \sigma_x^2/\log_2 M$ was the energy per bit, with $M = 4$. The five designs compared were the MMSE-VP design [3], the ImMMSE-VP scheme [10], the UCD-THP algorithm [6], and the GMD-MMSE-VP design [4], as well as our proposed UCD-MBER-VP design (please see Section I for a brief summary of these five designs). Only discrete-valued perturbation vectors were considered in the related designs. All the simulation results were averaged over 500 channel realizations.

Full-Rank System: First, we considered the case of $N = 3$ and $K = 3$. Assuming the availability of the CSI at both the transmitter and the receiver, the BER performance of the five designs is compared in Fig. 3. It can be seen that the two MUT designs, i.e., the ImMMSE-VP and the MMSE-VP, had a similar BER performance for this full-rank system, whereas the GMD-MMSE-VP transceiver design outperformed these two MUT preprocessing designs by 0.8 dB at the BER level of 10^{-5}. Although the UCD-THP transceiver design achieved the best performance at low SNR values, its performance significantly degraded at high SNRs and was outperformed by all the other designs. It can also be seen from Fig. 3 that the proposed UCD-MBER-VP transceiver design achieved a 2-dB SNR gain at the target BER of 10^{-5} over the GMD-MMSE-VP.

The robustness of all the five algorithms against the channel estimation error (CEE) was investigated next. A complex-valued Gaussian white noise with variance 0.01 was added to each channel tap $h_{i,k}$ to represent the CEE at both the transmitter and the receiver, and the BERs of the five designs under this CEE were depicted in Fig. 4. It can be seen that the performances of the five designs were all degraded. In particular, the UCD-THP scheme was seen to be very sensitive to CEE and completely broke down. It can also be seen from Fig. 4 that the proposed UCD-MBER-VP design was no more sensitive to CEE than the other benchmark designs, and it maintained the best BER performance.

Rank-Deficient System: The system was then configured to use $N = 2$ transmit and $K = 4$ receive antennas for 4 4-QAM users,

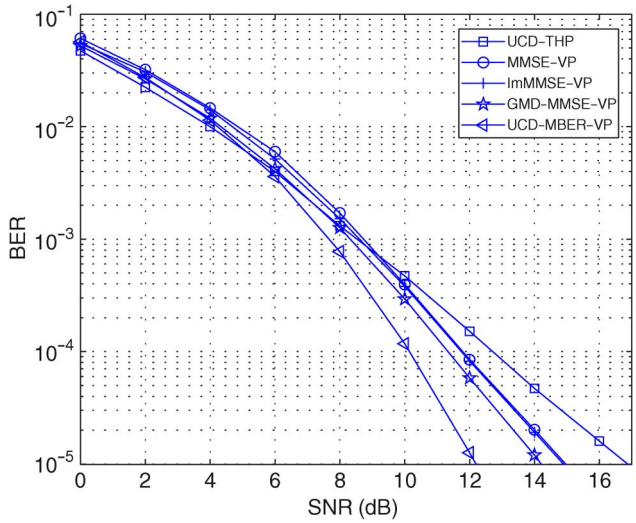

Fig. 3. BER performance comparison of the UCD-THP design [6], the MMSE-VP design [3], the ImMMSE-VP design [10], the GMD-MMSE-VP design [4], and our proposed UCD-MBER-VP design for communicating over flat Rayleigh fading channels using $N = 3$ transmit antennas and $K = 3$ receive antennas to support $K = 3$ 4-QAM users, assuming perfect CSI.

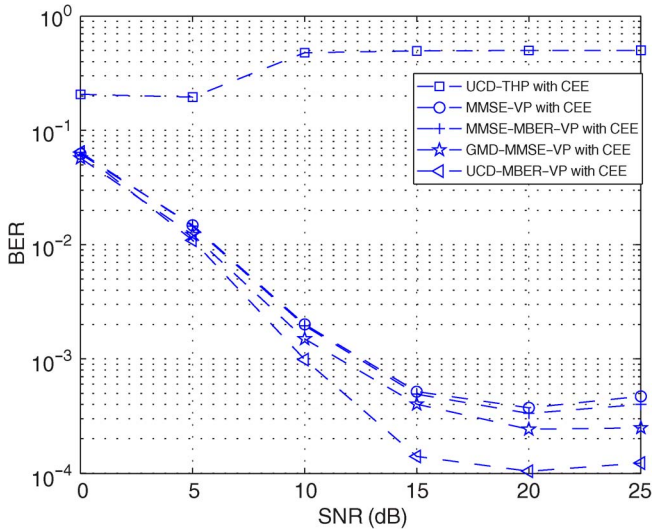

Fig. 4. BER performance comparison of the UCD-THP design [6], the MMSE-VP design [3], the ImMMSE-VP design [10], the GMD-MMSE-VP design [4], and our proposed UCD-MBER-VP design for communicating over flat Rayleigh fading channels using $N = 3$ transmit antennas and $K = 3$ receive antennas to support $K = 3$ 4-QAM users, assuming imperfect CSI with CEE.

which was a challenging rank-deficient scenario. The BERs of the five designs assuming perfect knowledge of the CSI at both the transmitter and the receiver are shown in Fig. 5. The two joint transceiver designs, namely, the GMD-MMSE-VP and UCD-THP schemes, encountered high error floors, which showed that they were unable to differentiate the users' information in this demanding case. The MMSE-VP scheme showed a significantly better performance but still suffered from a visible error floor, as shown in Fig. 5. The ImMMSE-VP algorithm considerably outperformed the foregoing three designs and exhibited a much reduced error floor. By contrast, the proposed UCD-MBER-VP transceiver design outperformed the ImMMSE-VP design by about 10 dB at the target BER of 10^{-5}, and it did not exhibit an error floor. This showed its ability to successfully operate in the challenging rank-deficient scenario. The MMSE-VP, the ImMMSE-VP, and the

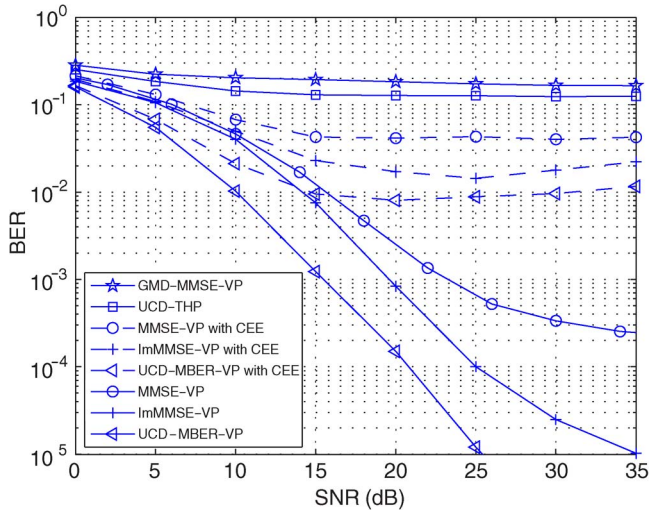

Fig. 5. BER performance comparison of the GMD-MMSE-VP design [4], the UCD-THP design [6], the MMSE-VP design [3], the ImMMSE-VP scheme [10], and our proposed UCD-MBER-VP design for communicating over flat Rayleigh fading channels using $N = 2$ transmit antennas and $K = 4$ receive antennas to support $K = 4$ 4-QAM users, assuming perfect CSI (solid curves) and imperfect CSI with CEE (dashed curves).

UCD-MBER-VP were then tested under the same CEE condition as specified in the previous example, and their BERs obtained under this CEE are also shown in Fig. 5. It can be seen that the effect of CEE was more serious in the rank-deficient case. Again, the UCD-MBER-VP design achieved the best BER performance, and it was no more sensitive to CEE than the other two benchmark schemes.

V. Conclusion

We have proposed a joint transceiver design based on the UCD and MBER vector perturbation. In this UCD-MBER-VP design, the precoding and equalization matrices were calculated by the UCD, whereas the perturbation vector was chosen based on the MBER criterion. The BER performance of our proposed transceiver design was compared with four benchmark designs, including the MMSE-VP and ImMMSE-VP preprocessing schemes, as well as the UCD-THP and GMD-MMSE-VP joint transceiver designs. The results obtained demonstrated that the novel UCD-MBER-VP design considerably outperforms these benchmark schemes, particularly in the challenging rank-deficient scenario. Our proposed UCD-MBER-VP design has also been shown to have a similar complexity with those of the GMD-MMSE-VP, MMSE-VP, and ImMMSE-VP designs.

References

[1] L. Hanzo, O. Alamri, M. El-Hajjar, and N. Wu, *Near-Capacity Multi-Functional MIMO Systems: Sphere-Packing, Iterative Detection, and Cooperation*, 1st ed. New York: Wiley, 2009.

[2] S. Chen, W. Yao, and L. Hanzo, "Semi-blind adaptive spatial equalization for MIMO systems with high-order QAM signalling," *IEEE Trans. Wireless Commun.*, vol. 7, no. 11, pp. 4486–4491, Nov. 2008.

[3] D. A. Schmidt, M. Joham, and W. Utschick, "Minimum mean square error vector precoding," in *Proc. PIMRC*, Berlin, Germany, Sep. 11–14, 2005, vol. 1, pp. 107–111.

[4] F. Liu, L. Jiang, and C. He, "Joint MMSE vector precoding based on GMD method for MIMO systems," *IEICE Trans. Commun.*, vol. E90-B, no. 9, pp. 2617–2620, Sep. 2007.

[5] Y. Jiang, J. Li, and W. Hager, "Joint transceiver design for MIMO communications using geometric mean decomposition," *IEEE Trans. Signal Process.*, vol. 53, no. 10, pp. 3791–3803, Oct. 2005.

[6] Y. Jiang, J. Li, and W. Hager, "Uniform channel decomposition for MIMO communications," *IEEE Trans. Signal Process.*, vol. 53, no. 11, pp. 4283–4294, Nov. 2005.

[7] M. Tomlinson, "New automatic equaliser employing modulo arithmetic," *Electron. Lett.*, vol. 7, no. 5, pp. 138–139, Mar. 1971.
[8] M. Costa, "Writing on dirty paper," *IEEE Trans. Inf. Theory*, vol. IT-29, no. 3, pp. 439–441, May 1983.
[9] B. M. Hochwald, C. B. Peel, and A. L. Swindlehurst, "A vector-perturbation technique for near-capacity multiantenna multiuser communication—Part II: Perturbation," *IEEE Trans. Commun.*, vol. 53, no. 3, pp. 537–544, Mar. 2005.
[10] W. Yao, S. Chen, and L. Hanzo, "Improved MMSE vector precoding based on MBER criterion," in *Proc. VTC Spring*, Barcelona, Spain, Apr. 26–29, 2009.
[11] R. Habendorf and G. Fettweis, "Vector precoding with bounded complexity," in *Proc. SPAWC*, Helsinki, Finland, Jun. 17–20, 2007, pp. 1–5.
[12] U. P. Rico, E. Alsusa, and C. Masouros, "A fast least-squares solution-seeker algorithm for vector-perturbation," in *Proc. GLOBECOM*, New Orleans, LA, Nov. 30–Dec.4, 2008, pp. 1–5.
[13] R. Habendorf and G. Fettweis, "Nonlinear optimization for the multiuser downlink," in *Proc. EW*, Paris, France, Apr. 1–4, 2007, pp. 1–7.
[14] F. Liu, L. Jiang, and C. He, "Low complexity MMSE vector precoding using lattice reduction for MIMO systems," in *Proc. ICC*, Glasgow, U.K., Jun. 24–28, 2007, pp. 2598–2603.
[15] S. Chen, A. Livingstone, H.-Q. Du, and L. Hanzo, "Adaptive minimum symbol error rate beamforming assisted detection for quadrature amplitude modulation," *IEEE Trans. Wireless Commun.*, vol. 7, no. 4, pp. 1140–1145, Apr. 2008.
[16] G. H. Golub and C. F. Van Loan, *Matrix Computations*. Baltimore, MD: The Johns Hopkins Univ. Press, 1983.
[17] I. E. Telatar, "Capacity of multi-antenna Gaussian channels," *Eur. Trans. Telecommun.*, vol. 10, no. 6, pp. 585–595, Nov./Dec. 1999.
[18] S. Tan, "Minimum error rate beamforming transceivers," Ph.D. dissertation, School Electron. Comput. Sci., Univ. Southampton, Southampton, U.K., Apr. 2008.